Advances in Engineering Software 185 (2023) 103514

Contents lists available at ScienceDirect

Advances in Engineering Software

journal homepage: www.elsevier.com/locate/advengsoft

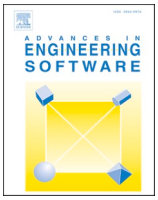

Parametric nonlinear modelling of 3D masonry arch bridges

S. Grosman *, L. Macorini, B.A. Izzuddin

Department of Civil and Environmental Engineering, Imperial College London, United Kingdom

ARTICLE INFO

Keywords:
Masonry arch bridges
Parametric modelling
Rhino-grasshopper

ABSTRACT

Detailed modelling of masonry arch bridges and viaducts presents unique computational challenges. Not only do such structures exhibit complex nonlinear behaviour, but they are also difficult to describe within a consistent computational framework for high-fidelity simulations, due to the range of interactive components with varying geometric characteristics. This paper presents a novel parametric model design tool for the generation of detailed 3D FE meshes of realistic masonry arch bridges and viaducts. This tool has been developed according to a modular description as an add-on component within the Rhino – Grasshopper environment. It allows for modular complex bridge assemblages with independent definition of the key viaduct parts, including arch barrels, spandrel walls, piers as well as multi-layered fill. Moreover, new parts can be seamlessly introduced into the framework due to its modular nature. Notably, as all components are geometrically addressable, it is possible to further enhance the model generation tool by adding non-standard routines to create more complex geometry than that allowed by the current parametric definition. Importantly, the developed strategy enables variable fidelity model generation, where different segments of an analysed viaduct can be represented by meso- and/or macro-scale masonry descriptions at different levels of detail. This approach further enables the consideration of initial damage in the brick/blockwork, which is a very common feature of many existing masonry bridges and viaducts.

1. Introduction

The advent of the 18th and 19th century industrial revolution and the subsequent economic growth promoted large scale construction of masonry arch bridges and viaducts in the UK and around Europe which are still in use at present. The age of these structures associated with the deterioration of the original masonry materials necessitates an accurate assessment of their performance under ever increasing traffic loading.

Different assessment methodologies for masonry arch bridges have been proposed in the past few decades. These approaches can be divided into three main categories: semi-empirical methods [1], equilibrium based methods [2,3] and detailed solid mechanics computational methods utilising Finite Element (FE) [4] or the Discrete Element [5] procedures. In current assessment practice, computational approaches considering a 2D representation of the bridge structure [6] are typically used. However, some recent studies [7,8] indicate that the three-dimensional nature of the bridge response cannot be adequately captured with reduced dimension models, thus paving the way for the use of detailed 3D descriptions leading to improved predictions under different loading conditions.

Detailed modelling of masonry arch bridges presents unique computational challenges. Not only do such structures exhibit complex nonlinear behaviour, but they are also difficult to describe within a consistent 3D computational framework for high-fidelity simulations, due to the range of interactive components with varying geometric characteristics.

When generating high-fidelity numerical models for masonry arch bridges and viaducts, it is vital to accurately represent all the structural and non-structural components in detail. The primary structural parts are the arch barrels that may be formed by several interconnected rings. Backfill and backing are supported by the main arches enabling the spread of load from the top rail or roadway. Spandrel walls are connected to the arches and piers and ensure lateral retainment of backfill and backing. Vertical loads are transferred via abutments and piers to the bridge foundations (Fig. 1).

When using detailed 3D mesoscale descriptions for the analysis of masonry bridges and viaducts, generic computer-aided design (CAD) software packages might be potentially employed for automatic mesh generation. However, their use is prevented by the difficulty of ensuring that the generated meshes comply with the actual bond of the masonry

* Corresponding author.
E-mail address: s.grosman15@ic.ac.uk (S. Grosman).

https://doi.org/10.1016/j.advengsoft.2023.103514
Received 21 December 2022; Received in revised form 20 April 2023; Accepted 13 June 2023
Available online 7 July 2023

parts of the bridge. This issue is exacerbated if it is necessary to introduce interface elements not only to connect adjacent brick/block units, but also between distinctive but interactive components to represent the physical interfaces between the different structural and non-structural domains. Furthermore, overly refined or incompatible meshes may be generated in the case of complex geometries.

Recently, novel model generation methods for masonry bridges utilising 3D point clouds and high-resolution photography have been proposed [9,10]. While these approaches show significant potential, they still require further refinement to reduce the amount of work involved in the model generation. It is also worth pointing out that sometimes computational models generated with such approaches can become impractical due to the excessive large number of elements involved.

Some preliminary work on the utilisation of generative algorithms to create mesoscale masonry models in a parametric fashion was presented in [11], where curved masonry wall models were developed accounting for manufacturing constraints. Further refinements are reported in [12], where the LiABlock_3D software for the limit equilibrium analysis of masonry structures is introduced. This program utilises graphics exported from CAD software packages as an assembly of polyhedral shapes. While efficient, such an approach for model generation is not practical when applied to large structures, as it requires significant refinements inside the CAD software.

An even further improvement to the above method was suggested by [13], where the parametric nature of the Grasshopper for Rhino software was utilised to construct block assemblages to be used to develop meshes for generic structural analysis codes.

This paper presents a novel parametric design tool for the generation of detailed 3D FE multi-scale meshes for realistic masonry bridges and viaducts. The current development employs the advanced nonlinear finite element analysis program ADAPTIC [14] for mesoscale and macroscale modelling of masonry structures, though the presented concepts are general and can be potentially applied to other FE programs presenting such modelling capabilities. The proposed approach for automatic mesh generation has been developed according to a modular description as an add-on component within the Rhino – Grasshopper environment [15]. In the following, a detailed description of the developed meshing strategy is provided. Subsequent numerical examples showcase the potential of the proposed approach for high-fidelity simulations of realistic masonry bridges and viaducts.

2. Modelling strategies for high-fidelity simulations of masonry bridges and viaducts

This paper focuses on the development of FE bridge and viaduct models for high-fidelity 3D simulations. In particular it capitalizes on prior work by the authors [7] where two distinct modelling strategies (meso and macroscale) were presented. In the macroscale modelling strategy, the masonry components of a viaduct are modelled using continuum 3D solid elements, whose size is independent from the dimensions of units and mortar joints leading to computationally efficient 3D models. The material description within this framework is based upon a constitutive model combining the concepts of plasticity and damage assuming masonry as a single constituent. Such a combination has proven to be effective in capturing both irreversible deformations and the deterioration of stiffness in quasi-brittle materials. These constitutive models [16,17] are employed for a homogenised continuum representation of the masonry in arch bridges, hence appropriate interpretation is needed to relate the results to the nature of the real material, comprising distinct constituents (e.g. masonry units and mortar joints). In general, while the reduction of the modelled material to a single constituent guarantees computational benefits enabling the nonlinear simulations of large structures, it requires calibration of the material parameters based upon physical experiments on large components, or the use of homogenisation techniques and the results from material tests on masonry constituents (e.g. bricks and mortar joints).

In the adopted mesoscale description on the other hand, the masonry material is modelled based on separate representations for brick units and mortar joints. More specifically, as elaborated in [18], elastic quadratic solid elements are used to describe units and nonlinear quadratic interface elements to represent mortar joints and potential fracture surfaces within bricks. The material description for nonlinear interfaces employs a cohesive-frictional constitutive model [19], providing computationally robust solutions of the local nonlinear problem. A multi-surface yield criterion in the stress domain is adopted, while the degradation of strength and stiffness is captured through the evolution of an anisotropic damage tensor which is coupled with the plastic work. Importantly, mesoscale material parameters can be obtained by small scale tests on individual components as in [20] and also via inverse analysis based on low-invasive in-situ experiments. The adopted masonry mesoscale strategy has been recently applied to represent single- and multi-ring arches in isolation [21,22] and to investigate the response of small single-span and multi-span bridges [23,24]. However, the high computational cost hinders the direct use of this approach for nonlinear analysis of large masonry viaducts.

A substantial amount of research involved macroscale modelling of both single [25] and multi-span bridges [26]. Further refinements can be seen in works where mesoscale descriptions are utilised for the arches and macroscale models for the spandrel walls [,25,27]. However, there is a clear lack of research where detailed mesoscale modelling is applied to both arch barrels and spandrel walls of realistic bridge structures. This can be attributed to the highly involved and time-consuming process of 3D model generation. To address this issue, it is possible to utilise

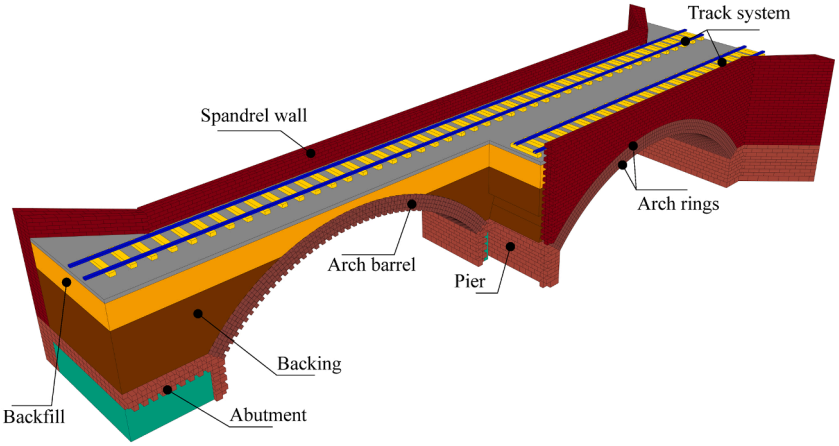

Fig. 1. Masonry arch bridge composition.

generative algorithms, as the 3D mesh generation strategy presented below, to automate the development of the 3D high-fidelity models.

3. 3D mesh generation strategy

To effectively model realistic arch bridges parametrically, the developed mesh generation tool treats each structural and non-structural part as an independent entity that can be interfaced. Current developed components include arch barrels (AB), backing/backfill (BKFL), spandrel walls (SW), and piers (PR).

The Arch Barrel (AB) component is designed to represent various brick and block-masonry arch barrels. In the AB parametric definition, three arch shapes are accounted for: segmental, parabolic, and free-form. The free-form definition is achieved by supplying the necessary arch curve directly to the AB component leading to a higher versatility of the modelling tools (i.e. it can be employed for modelling non-smooth arches). Segmental and parabolic shapes represent a subset of free-form arches, but they are intentionally segregated as they are the most common types.

The shape of the arch intrados is used to generate the mesh of the arch barrel. To this end, the intrados curve is first divided in two parts at the apex, and then each of the resulting components is subdivided further into segments taking into account the specific brick/block dimensions and the masonry bond. These points are then projected along the normal to the intrados curve to form the brick layer geometry. In case of discontinuity in the arch curve, special consideration is taken to define the key stone segments.

The masonry arch generation procedure considers multiple predefined bond patterns (e.g. runing, English, stretcher (Fig. 2a, b, c)). Each pattern is a layered 3D structure that is characterised by repeatability in every direction of the bond plane (Fig. 2d). It is worth noting that, although the bond pattern is repeatable in each of the constituent layer planes, it is usually cyclic in the out of plane direction (Fig. 2d).

Number of layers in each pattern cycle is unique for each bond type. Another important characteristic of every pattern is the shift size (Fig. 2a) with most common shift sizes being either a quarter or half of the brick length. Considering all the above, a way to uniquely describe every bond pattern was defined and implemented for all masonry components (AB, SW and PR).

Each bond pattern can be represented with the ``bond seed", which corresponds to a 3D matrix containing the smallest fragment of the bond pattern that can be replicated in any direction to create a 3D mesoscale mesh for the specific masonry bond. Every brick in the ``bond seed" is represented with a unique number that can also indicate the brick spatial orientation (i.e., numbers 0 to 9 representing bricks with largest side aligned horizontally while numbers 10 to 19 indicating bricks aligned vertically). Identical numbers indicate that adjacent elements represent the same brick and, different numbers on the other hand indicate presence of the mortar joint. (Fig. 2e).

Most of the mesh connectivity (relationship on what elements share adjacent side) for the masonry structure can be represented as a 3D array. Replicating the ``bond seed" over the mesh domain and then going over each of the unique element interfaces it is possible to establish any bond for any given mesh, where rectangular hexahedral elements are prevalent (Fig. 3).

The Backfill / backing (BKFL) component is designed to represent the

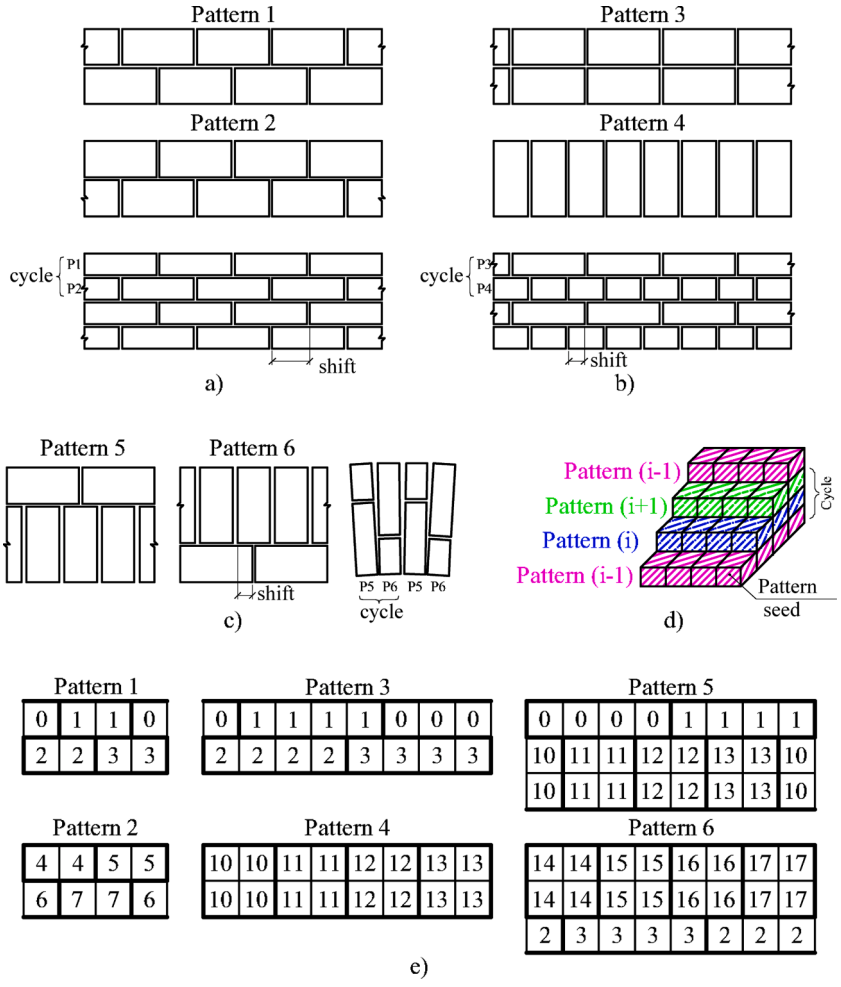

Fig. 2. Bond pattern definitions: a) running bond; b) English bond; c) stretcher bond; d) 3D bond structure; e) ``Bond seed" definitions.

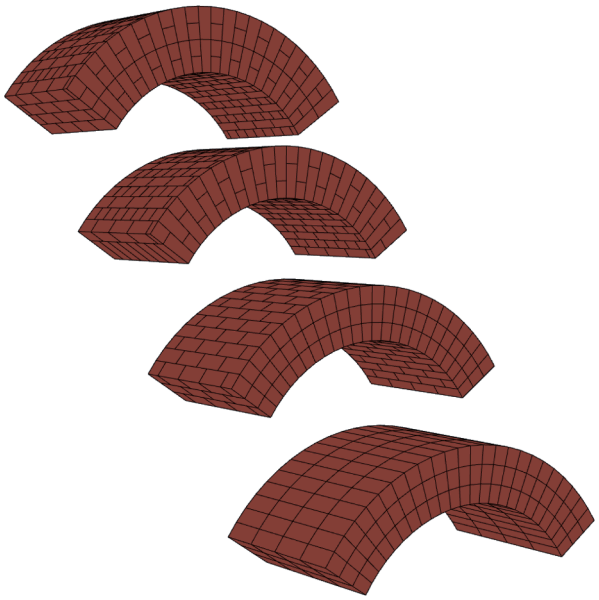

Fig. 3. Different bond patterns for arch barrels.

typical layered structure of bridge filling. This component is generated based on the extrados input from the AB component and information about the constituent layers of the fill (e.g. backing, backfill, ballast (Fig. 4a). The developed tool enables the BKFL component to be meshed with either structured hexahedral elements or free-form triangular prisms. BKFL component also allows for interface generation between different layers.

The mesh for the BKFL component is developedvia extrusion from the planar mesh constructed on the side of the fill. Structured mesh is generated by subdividing irregularly shaped planar segment into the four-sided segments, where all opposing sides have the same number of mesh divisions (specified as Nx[i] for horizontal and Ny[j] for vertical divisions in Fig. 4b). As planar meshing is independent from extrusion, different meshing approaches can be easily accommodated. This component can be also utilised for the case of skew bridges, as it considers an extrusion vector which can be not orthogonal to the arch face.

The BKFL component is attached to the arch barrel via a non-conforming mesh interface that can be reduced to the connectivity via standard interface elements for scenarios where mesh compatibility is achieved. The developed tool also allows for a fine control over meshing in the out of plane direction to accommodate loading from traffic.

The spandrel wall (SW) component is developed based on the BKFL component, and it is provided with meso-scale capabilities. This feature facilitates seamless connectivity between SW and BKFL components, which can be achieved by direct interface element connectivity or non-conforming mesh connectivity. The latter option is used to connect mesoscale SW to BKFL, while the former can be employed for macro-scale modelling at varying levels of fidelity.

To this end, a modification of the previously described meshing algorithm was devised. Initially the planar bounding box of the spandrel wall is discretized with a regular mesh, then the elements that overlap with the arch barrel extrados, are morphed to follow the arch curve, with inclusion of triangular elements where necessary. Finally, the elements not associated with the spandrel wall are removed, and the planar mesh is extruded in accordance with the mesh size (Fig. 5). SW components also benefit from the previously described bond generation strategy.

The pier (PR) component is used to model different pier and abutment structures. It is designed to have a varied number of internal and external layers with specific material properties (Fig. 6a, the layer size is denoted S1, S2, S[*i*]). Due to modularity, the PR component only represents half of the actual pier and the whole pier is generated when adjacent spans are joined together (Fig. 6b). The developed PR component accounts for the possibility of different materials being used for different parts of the actual pier (e.g. piers with internal filling materials). The geometry of each component is uniquely defined from the previously described AB, BKFL, and a set of two SW components supplemented with sizing information of the pier. To account for a large variety of possible pier internal structures a robust approach to mixing meso- and macroscale modelling strategies was implemented, where not only each individual layer can be assigned to a specific modelling fidelity level, but also all layers between them can be treated independently.

Mesh generation for PR component is not dissimilar from the strategy described before for the SW component, where the initial generation of regular rectangular mesh is then morphed to fit the actual geometry. It is worth noting that specific bond definition for PR is a more involved process. This can be attributed to the fact that all previously defined structural components can be generated geometrically and also notionally (arch and walls remain made out of bricks following the same pattern) via extrusion along the bridge width, piers on the other hand due to the specific construction features are more complex and cannot be

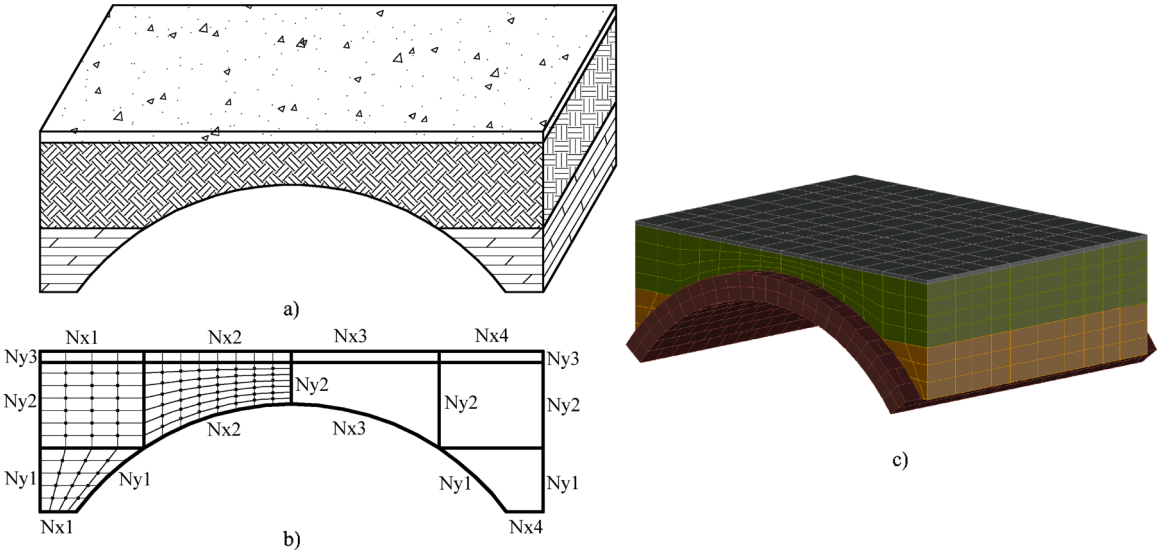

Fig. 4. BKFL component: a) Layered structure; b) Meshing strategy; c) Meshed component with different layers.

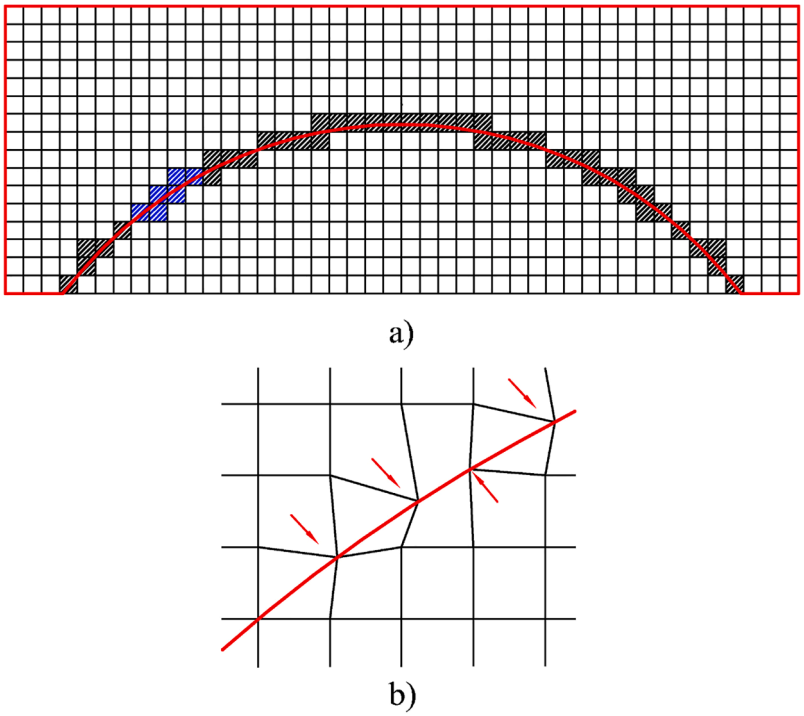

Fig. 5. Mesh morphing for the SW component: a) Initial regular mesh and overlapping segments; b) Mesh morphing strategy.

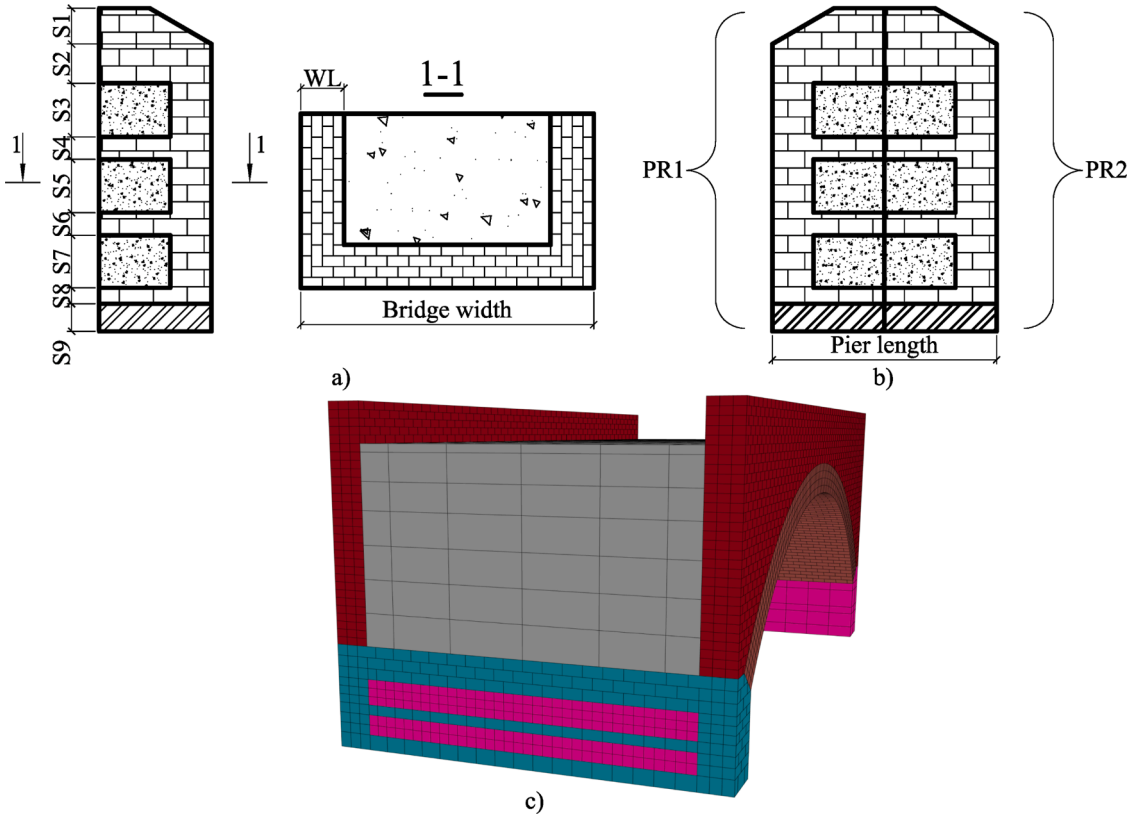

Fig. 6. PR component model: a) Pier detail; b) Pier assembly; c) Meshed model.

treated the same way (external brick layer always surrounds the internal one). To this end all elements in the pier component are assigned not only regular numbers but also radial and circular indexes, where the radial index indicates the layer of brick, and the circular index specifies the element position in the current set. This indexing in addition to usual geometric indexing enable the application of the bond seed matrix to a more complex structural configuration such as actual piers. It is worth noting that this efficiency in modelling masonry comes at the expense of

a more simplistic approach to the corner bond compared to what can be observed in the actual structures, nevertheless this simplification is unlikely to greatly affect the overall structural response prediction.

Span construction (Fig. 7) is organized based on the following hierarchy: $SPN = AB \rightarrow BKFL \rightarrow SW \times 2 \rightarrow PR \times 2$.

Any component except for the arch barrel can be removed from the generated span. To simplify the generation of each individual span for multi-span applications, all spans can be modelled at the initial position, and then translated to their actual position via a dedicated TRANSLATION component.

The final bridge is constructed as a combination of several spans (Fig. 7). Different components are in turn joined at the interfaces. Three connectivity strategies are allowed. If the interfaces of two adjacent components match perfectly, nodes at the boundary are merged, as for the span-to-span interface of neighbouring backfill sections. On the other hand, if potential separation between contiguous parts needs to be represented, a layer with nonlinear interfaces is generated between them (e.g. spandrel wall to backfill interface). The final option comes into play when there is no match between the mesh of adjoining components; in this case, the two parts are connected by mesh tying [28].

The developed tool also contains capabilities for generation of the curved bridges and viaducts. This is achieved via a MORPH component that takes the desired bridge longitudinal axis in form a spline curve, and then maps the straight bridge geometry onto the curved path generating the desired bridge/viaduct curvature (Fig. 8).

To enable independent mesh characteristics for the different parts of a masonry bridge model and enhance computational efficiency, a mesh tying strategy [28] based on the mortar method is employed. At the physical interfaces between the bridge components (e.g. arch, lateral walls and backfill) master and slave surfaces (Fig. 9) are defined, where the slave surfaces are associated with the coarser mesh (backfill domain), which is typically connected to the adjacent finer mesh, representing a different masonry part of the bridge, by nonlinear interfaces to model potential sliding and separation at the physical interface. The described interface surfaces do not need to be planar; they may intersect each other, and they allow for separate material description by assigning distinct sets of material parameters for each surface independently.

Detailed 3D modelling of large and complex structural systems such as realistic masonry arch bridges entails the use of a large number of degrees of freedom (DOFs), which renders the solution of the nonlinear problem impractical, especially when using standard computation resources. Computationally efficiency can be dramatically improved by parallel computation. In previous research [29] large computer clusters with more than 130,000 cores were adopted for implicit dynamic simulation of large linear FE models (200 million DoF) leading to a significant speed-up of the numerical simulations. Similar improved efficiency was found in [30], where 65,000 cores were used for the solution of a model with 40 million DoFs. Both studies indicate that computational efficiency reduces when the number of cores exceeds a limit value and the computing time becomes dominated by intercommunication between nodes. A different approach to scalability is presented in [31] and [32], where improved iterative solver algorithms are presented and applied to the solution of the different complex FE problems. To fully utilise the computational benefits associated with modern computer architecture and improve computational efficiency, a domain decomposition approach developed previously at Imperial College [33] is utilised in the proposed modelling strategy for masonry bridges and viaducts. According to this strategy, a large structure is divided into partitions (Fig. 10) corresponding to subdomains of the original structure and a ``parent structure'', which is composed of dual super-elements. Each super-element consists of the boundary nodes of an individual partition and accounts for the two-way communication of the subdomain with the parent structure, which allows the parallelisation of the analysis, where each part is solved by a dedicated computer core in a dedicated memory segment. In previous research, this computational strategy was effectively used in mesoscale simulations of masonry components [34] including arches [21] and bridges [23,35] leading to a significant reduction of the computing time, which can be further reduced with the adoption of mixed-dimensional coupling [36] albeit with minor consequent reduction in accuracy [21].

Another useful feature of the developed tool is the ability to address individual mesh elements based on their geometric location. This feature allows a straightforward definition of pre-existing structural damage (e.g. cracks) by setting material properties of the interfaces associated with an actual crack geometry with lower strength parameters. Alternatively, a similar approach can be used to selectively reduce properties of solid elements for macro-scale model or completely remove solid elements from the mesoscale model to account for brick loss in real structures.

4. Numerical applications

Numerical examples are presented to showcase the potential of the proposed high-fidelity modelling strategy for masonry bridges and viaducts, utilising the advanced nonlinear finite element analysis program ADAPTIC [14]. Initial focus is placed on the effects of existing damage in the masonry material of key structural components. Then the effectiveness of different partitioning strategies to improve computational

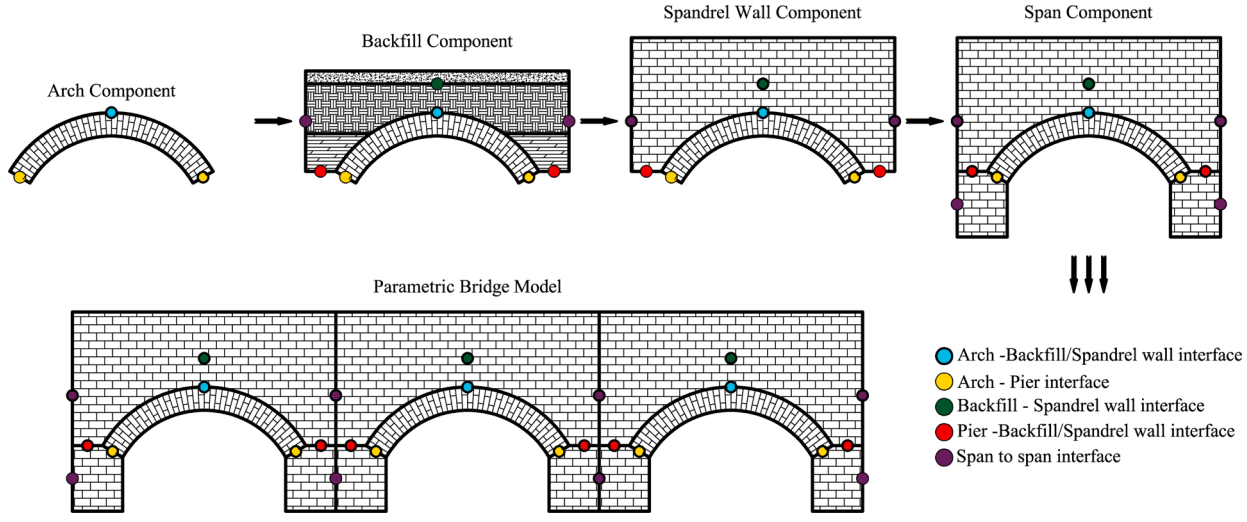

Fig. 7. Modular design for the structural components.

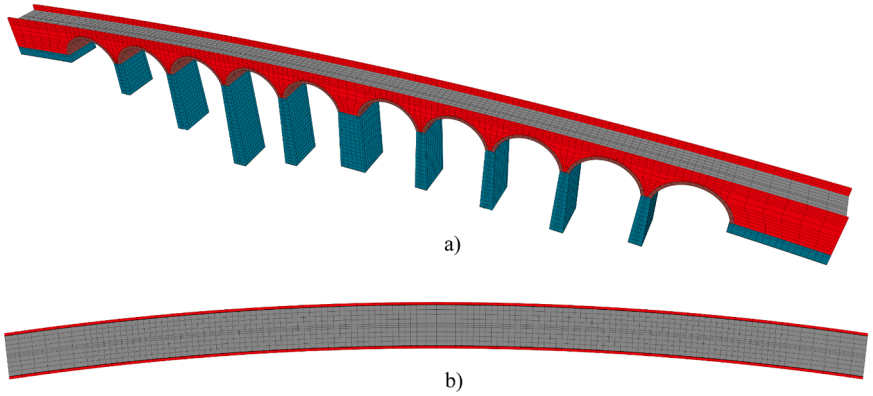

Fig. 8. Curved viaduct a) 3D and b) plan view.

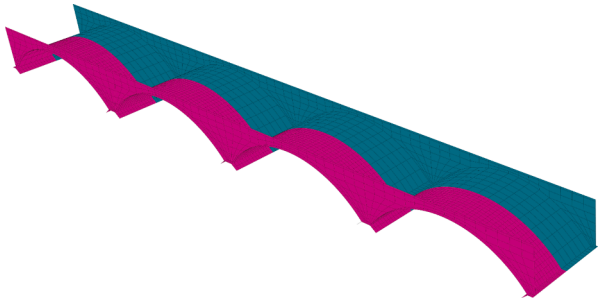

Fig. 9. Master (cyan colour) and slave (magenta colour) surfaces for the mesh tying algorithm applied to a masonry viaduct model.

efficiency is investigated.

4.1. Effects due to existing damage in the brick/blockwork

A five span viaduct has been modelled utilising a mixed meso/macro strategy (Fig. 11). According to this modelling approach, a small portion of a large viaduct corresponding to a single span or to an individual brick/block-masonry component (e.g. arch or spandrel wall) within a span is modelled using a detailed mesoscale description to capture local effects, while the rest of the structure is represented by an efficient macroscale model, which significantly reduces the computational cost (Fig. 11a).

This modelling approach is used also to take into account the effects of existing cracking in the brickwork (Fig. 11b). In this case, cracks are explicitly represented in the mesoscale mesh, where nonlinear interfaces with negligible tensile strength and cohesion are introduced along the planes of cracking. By specifying a set of surfaces the developed algorithm then finds all mortar interfaces that are close or overlap with the supplied set and assigns ``damaged'' properties to them. The developed meshing tool can support both straight and curved surfaces as well as multi-segmented non-contiguous surfaces.

To illustrate the use of such advanced modelling capabilities that allow for initial cracking, numerical tests on a realistic viaduct with five spans (Fig. 11c) with and without damage were conducted. Some of the most typical damage patterns observed in real masonry arch barrels were considered. They include a transverse crack at quarter span and a longitudinal crack at quarter width, as shown in Fig. 12 with the brick pattern indicating regions where mesoscale definitions are used.

The structure is analysed under the effect of quasi static loading representative of a typical railway bogie (two forces spaced at 1800 mm applied over the size of the railway slipper) located between quarter and mid-span, as shown in Fig. 11a, c. Material properties used in the model are summarised in Table 1. Negligible tensile strength (f_t = 0.001 N/mm^2) and cohesion (c = 0.001 N/mm^2) are provided to the damaged mortar interfaces resulting in cracks opening from the start of the numerical simulation. On the other hand, damaged interfaces can still transfer compressive forces as well as friction between adjacent units, as the adopted constitutive relationship for mortar interfaces accurately represents crack opening, closure and shear frictional resistance.

Deformed shapes and representative load-displacement curves for all of the analysed cases are presented in Figs. 13 and 14.

The numerical results indicate that the assumed damage scenarios do not substantially affect the static capacity of the bridge. On the other hand, initial damage determines the stiffness and the deformed shape of the structure at collapse as shown in Fig. 13a-c. In particular substantial reduction in transverse stiffness can be observed for the case with longitudinal crack (Fig. 14). Obtained results are in good agreement with the findings reported in [37], where a similar strategy to take into account initial damage was adopted.

It is important to point out that the mixed model presented in Fig. 11 can be readily used for parametric studies due to its improved

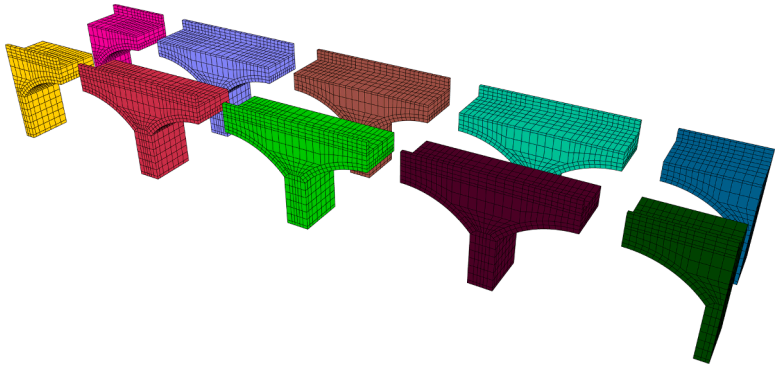

Fig. 10. Partitioning strategy for a masonry viaduct.

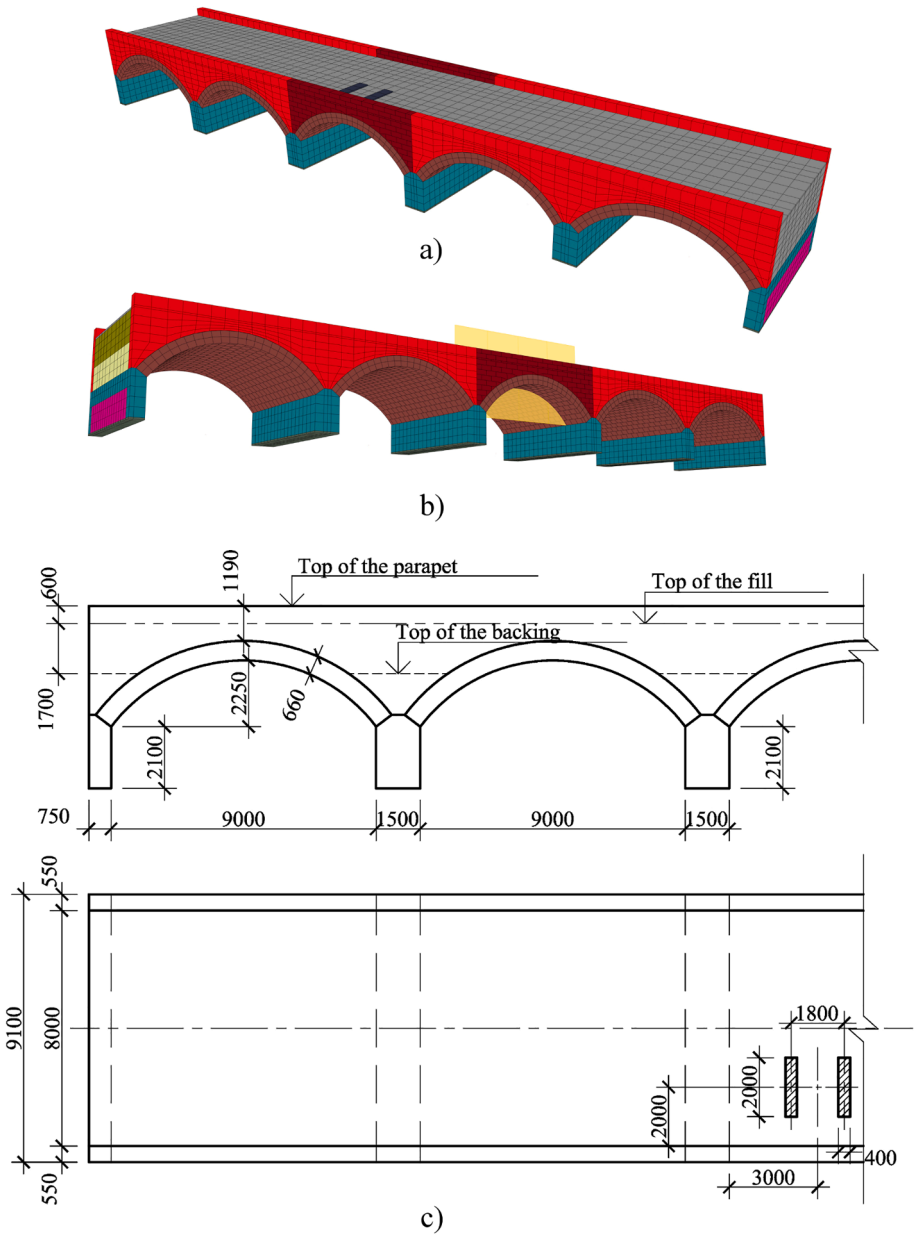

Fig. 11. Damage application procedure a) Mixed relaxed FE model; b) Damage plane; c) Dimensions of the bridge.

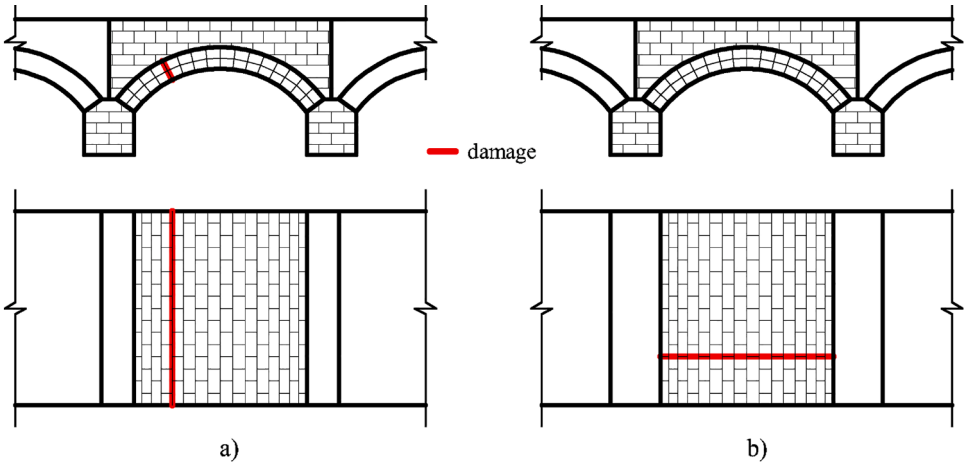

Fig. 12. Damaged scenarios: a) transverse crack; b) longitudinal crack.

Table 1
Material properties used in the analysis.

Bricks			
Young's modulus	E	N/mm^2	6000
Poison ratio	ν		0.15
Density	ρ	kg/m^3	2200
Mortar Interface			
Normal stiffness	K_n	N/mm^3	60
Tangent stiffness	K_t	N/mm^3	30
Tensile strength	f_t	N/mm^2	0.05
Friction angle	φ	rad	0.46
Cohesion	c	N/mm^2	0.085
Compressive strength	F_c	N/mm^2	9.1
Fracture energy [tension]	Gf_t	N*mm/mm^2	0.02
Fracture energy [shear]	Gf_s	N*mm/mm^2	0.125
Backing			
Young's modulus	E	N/mm^2	500
Poison ratio	ν		0.2
Density	ρ	kg/m^3	2200
Friction angle	φ	rad	0.76
Cohesion	c	N/mm^2	0.001

computational efficiency. Nevertheless, when investigating large multi-span bridges, it is paramount to employ an effective partitioning strategy for parallel computation, as described before, to achieve adequate computational performance.

4.2. Efficient partitioning schemes

To compare the improved efficiency guaranteed by different partitioning strategies, mesoscale simulations were performed considering the high-fidelity model for the 5-span viaduct shown in Fig. 15. The developed parametric tool allows for a straightforward definition of partitioning via specification of planes, that represent partitioning boundaries.

To simplify the scope of the assessment, only "effective" partitioning strategies were considered. In this context, "effective" refers to partitioning that does not result in overly large boundaries or segments that are too small or too large. Current investigation also considers hierarchic partitioning strategies [33,36], where each top partitioning level contains internal division. This approach is well suited for very large models where communication with child partitions becomes substantial. Thus, performance can be improved by reducing inter-node communication. Six basic division strategies are considered for the model as shown in Fig. 16.

In general, each division can be described by a sequence such as:6→4→3→2→0where the first number (6) indicates the division strategy (Fig. 16) at the lowest level of partitioning. The second number (4) and all the subsequent numbers (3,2) indicate the division strategy at a higher level of hierarchy. All descriptions terminate with zero, indicating that the model is fully assembled at the highest level of hierarchy. In this case, the lowest level structure is subdivided into 22 parts (Fig. 16– 6), each assigned to a CPU core. In the next stage, parts associated with the arch barrel, backfill and spandrel walls are assembled together into six parts (each on a dedicated CPU core) eliminating the DoFs associated with some of the internal boundaries (Fig. 16- 4). In the following stage (Fig. 16- 3) additional 6 cores are utilised to remove pier boundary. The penultimate stage seeks further boundary reduction (Fig. 16- 2) with the addition of 3 more cores, and finally the system is fully assembled (Fig. 16- 1) on the last core. Thus, a total number of 38 CPU cores is used for such a division strategy. Core usage for each strategy can be calculated from Fig. 16 by summing up unique segments from the encoding sequence (e.g. 22 + 6 + 6 + 3 + 1 for this case).

A numerical investigation was conducted considering the permutations of the six basic divisions strategies presented above to determine the optimal solution for bridge subdivision and nesting. To this end multiple models were run for one hour, then number of converged iterations were calculated for each model. The results (e.g. total number of iterations) normalised to the performance of the monolithic model (e.g. "0" in Fig. 16) are presented in Fig. 17. Normalisation was performed to make the results more general and reduce the effects of specific CPU architecture; for reference, the monolithic model utilising a single core solved 8 iterations of the considered nonlinear problem.

The obtained results indicate that the best performance is obtained

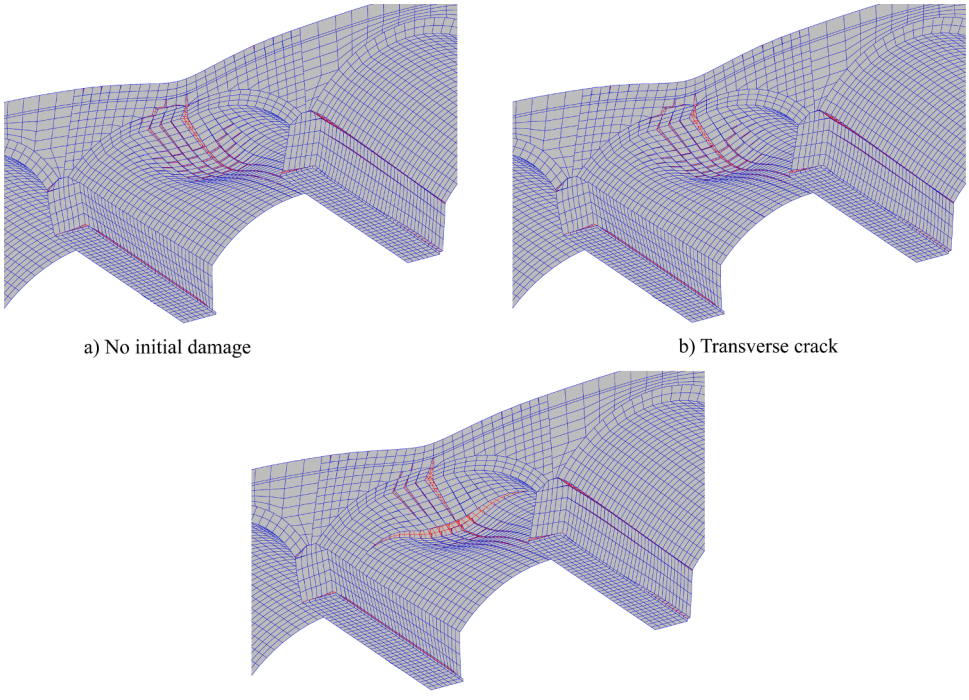

a) No initial damage

b) Transverse crack

c) Longitudinal crack

Fig. 13. Response of the pre-damaged structure.

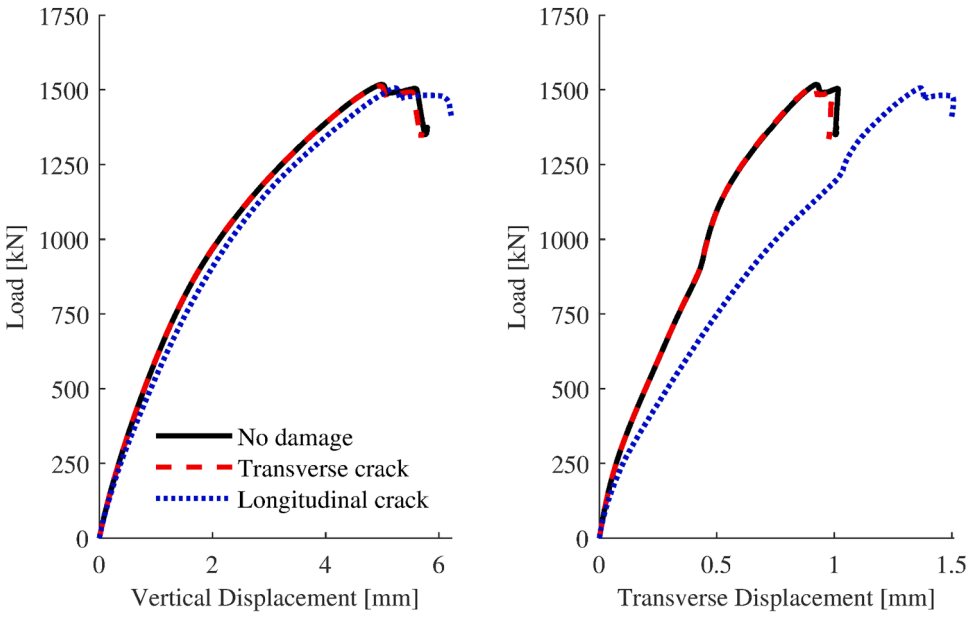

Fig. 14. Response curves for the damaged bridge.

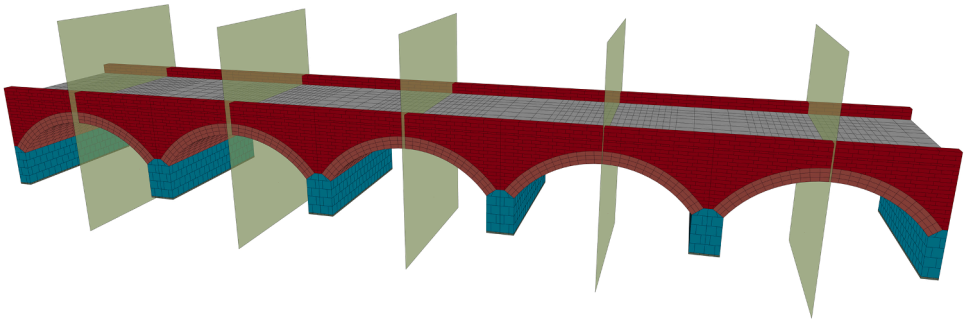

Fig. 15. Model employed for the assessment of different partitioning strategies (partition boundaries are defined by the vertical planes).

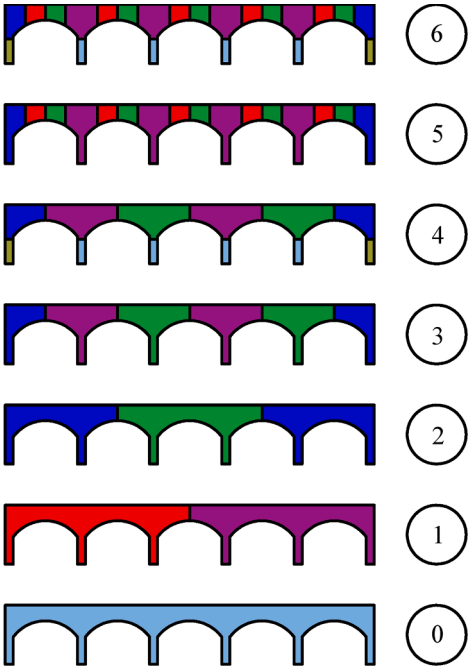

Fig. 16. Partitioning strategies at the lowest level.

for the hierarchic partitioning "6 → 3 → 0" (29 cores), where this model was found to be up to 13 times faster compared to the monolithic model "0" (1 core). Good performance was also observed for partitioning "5 → 1 → 0" (19 cores) and "5 → 3 → 0" (23 cores). Overall results highlight the improved efficiency of hierarchic partitioning, as 38% of best performing models utilise hierarchic partitioning with the best flat partitioning model achieving at most only 7.5 speed up compared to monolithic model, and a nearly 70% loss compared to the best hierarchic model. The numerical results also indicate that an overcomplicated hierarchic structure may lead to loss in performance, as such it can be concluded that maximisation of parent boundary reduction at every hierarchic step should be prioritised when devising an effective partitioning strategy. Results are also indicative of the fact that this particular model is only moderately scalable, as models associated with high number of cores (30+) achieve on average a reduced speedup factor of 6.

5. Conclusions

This paper presents a novel software tool developed in the Rhino – Grasshopper environment for parametric generation of high-fidelity models for masonry arch bridges and viaducts at meso- and macro-scale. The tool allows for modular definition of complex bridge assemblages with independent span definitions, utilising prior developments such as mesh-tying [28] and hierarchic partitioning [33,36] previously implemented in ADAPTIC [14], where the consideration of these

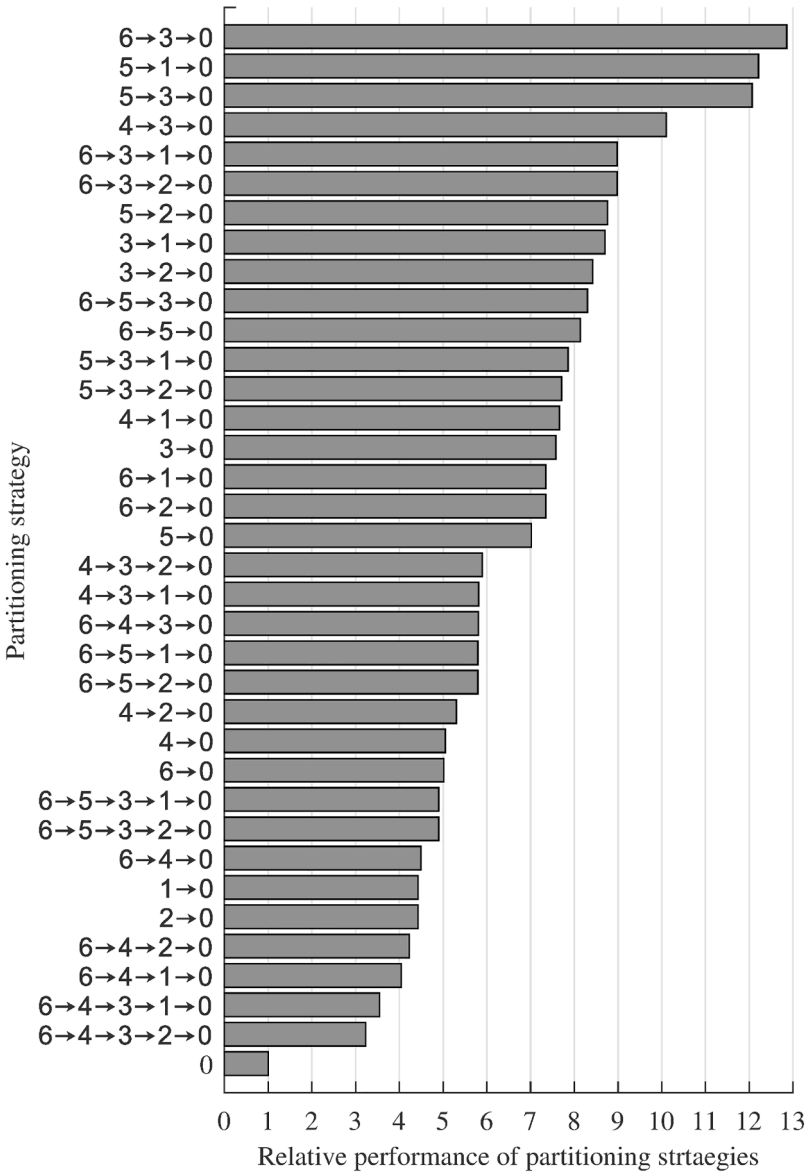

Fig. 17. Performance comparisons for different partitioning strategies.

techniques is seamlessly integrated into the parametric model generation.

New components enable the parametric definition of arch barrels, spandrel walls, piers as well as multi-layered fill. Moreover, additional components (e.g. skewed arches, end-walls, abutments, complex geometry pier-variants) can be seamlessly introduced into the framework, due to its modular nature.

The developed software tool also considers variable fidelity model generation, where different segments of the analysed structure can be represented using either meso- or macroscale representations. This approach further enables the consideration of initial damage in the brick/blockwork of each masonry part of the analysed structure.

In a first numerical example, a five-span bridge was analysed via a mixed fidelity model, considering also two scenarios with initial damage. The numerical results confirm applicability of the developed tool to the modelling of damaged structures with obtained results generally conforming to the data presented in [37]. A second numerical investigation addressed the problem of partitioning of large-scale bridge models for improved computational efficiency. A large family of possible partitions was assessed, and an optimal partitioning scheme was established. The results confirm the improved efficiency guaranteed by hierarchic partitioning and provide some general indications for the definition of effective partitioning strategies. Presented studies confirm the versatility of the developed tool and demonstrates that the developed strategy for automatic generation of complex numerical models is efficient, substantially (by an order of magnitude) reducing time required for generation of the computational models especially when considering variation studies where geometry changes between different options.

Future work will include the introduction of new components (e.g. internal spandrel walls, stepped structural elements) as well as an investigation of the effects of initial damage under cyclic loading conditions for realistic masonry bridges and viaducts, which has been made feasible through the modelling developments presented in this paper.

CRediT authorship contribution statement

S. Grosman: Conceptualization, Methodology, Software, Formal analysis, Writing – original draft. **L. Macorini:** Conceptualization, Data curation, Writing – review & editing, Supervision, Funding acquisition. **B.A. Izzuddin:** Conceptualization, Writing – review & editing, Supervision, Funding acquisition.

Declaration of Competing Interest

The authors declare that they have no known competing financial interests or personal relationships that could have appeared to influence the work reported in this paper.

Data availability

Data will be made available on request.

Acknowledgments

The authors would like to acknowledge the Engineering and Physical Sciences Research Council (EPSRC) for the financial support (Grant EP/T001607/1).

References

[1] Pippard AJS. The approximate estimation of safe loads on masonry bridges. In: The civil engineer in war. Thomas Telford Ltd; 1948. p. 365–72. https://doi.org/10.1680/ciwv1.45170.0021.
[2] Heyman J. The Masonry Arch. Cambridge, UK: Cambridge University Press; 1982.
[3] Gilbert M, Melbourne C. Rigid-block analysis of masonry structures. The Struct Eng 1994;72(21):356–61.
[4] Milani G, Lourenço PB. 3D non-linear behavior of masonry arch bridges. Comput Struct 2012;110–111:133–50. https://doi.org/10.1016/j.compstruc.2012.07.008.
[5] Pulatsu B, Erdogmus E, Lourenço PB. Simulation of masonry arch bridges using 3D discrete element modeling. RILEM Bookseries 2019;18:871–80. https://doi.org/10.1007/978-3-319-99441-3_94.
[6] De Santis S, de Felice G. A fibre beam-based approach for the evaluation of the seismic capacity of masonry arches. Earthq Eng Struct Dyn 2014;43(11):1661–81. https://doi.org/10.1002/eqe.2416.
[7] Grosman S, Bilbao AB, Macorini L, Izzuddin BA. Numerical modelling of three-dimensional masonry arch bridge structures. *Proc Inst Civ Eng - Eng Comput Mech* 2021;174(2):96–113. https://doi.org/10.1680/jencm.20.00028.
[8] Franck SA, Bretschneider N, Slowik V. Safety analysis of existing masonry arch bridges by nonlinear finite element simulations. Int J Damage Mech 2020;29(1):126–43. https://doi.org/10.1177/1056789519865995.
[9] Riveiro B, DeJong MJ, Conde B. Automated processing of large point clouds for structural health monitoring of masonry arch bridges. Autom Constr 2016;72:258–68. https://doi.org/10.1016/j.autcon.2016.02.009.
[10] Stavroulaki ME, Riveiro B, Drosopoulos GA, Solla M, Koutsianitis P, Stavroulakis GE. Modelling and strength evaluation of masonry bridges using terrestrial photogrammetry and finite elements. Adv Eng Softw 2016;101:136–48. https://doi.org/10.1016/j.advengsoft.2015.12.007.
[11] Cavieres A, Gentry R, Al-Haddad T. Rich knowledge parametric tools for concrete masonry design automation of preliminary structural analysis, detailing and specifications. In: 2009 26th International symposium on automation and robotics in construction, ISARC 2009; 2009. p. 544–52. https://doi.org/10.22260/ISARC2009/0065.
[12] Cascini L, Gagliardo R, Portioli F. LiABlock_3D: a software tool for collapse mechanism analysis of historic masonry structures. Int J Archit Herit 2020;14(1):75–94. https://doi.org/10.1080/15583058.2018.1509155.
[13] Savalle N, Mousavian E, Colombo C, Lourenço PB. Fast generative tool for masonry geometries. In: 14th Canadian masonry symposium; 2021. p. 11.
[14] Izzuddin BA. Nonlinear dynamic analysis of framed structures. Ph.D. Thesis. Imperial College, University of London; 1991.
[15] McNeel R. Associates, "Rhinoceros 3D, version 6.0. Robert McNeel Assoc.; 2010.
[16] Lee J, Fenves GL. Plastic-damage model for cyclic loading of concrete structures. J Eng Mech 1998;124(8):892–900. https://doi.org/10.1061/(ASCE)0733-9399(1998)124:8(892).
[17] Chisari C, Macorini L, Izzuddin BA. Multiscale model calibration by inverse analysis for nonlinear simulation of masonry structures under earthquake loading. Int J Multiscale Comput Eng 2020;18(2):241–63. https://doi.org/10.1615/IntJMultCompEng.2020031740.
[18] Macorini L, Izzuddin BA. A non-linear interface element for 3D mesoscale analysis of brick-masonry structures. Int J Numer Methods Eng 2011;85(12):1584–608. https://doi.org/10.1002/nme.3046.
[19] Minga E, Macorini L, Izzuddin BA. A 3D mesoscale damage-plasticity approach for masonry structures under cyclic loading. Meccanica 2018;53(7):1591–611. https://doi.org/10.1007/s11012-017-0793-z.
[20] CUR. Structural masonry: a experimental/numerical basis for practical design rules. CUR, Gouda, The Netherlands; 1994. Report 171.
[21] Zhang Y, Macorini L, Izzuddin BA. Mesoscale partitioned analysis of brick-masonry arches. Eng Struct 2016;124:142–66. https://doi.org/10.1016/j.engstruct.2016.05.046.
[22] Zhang Y, Macorini L, Izzuddin BA. Numerical investigation of arches in brick-masonry bridges. Struct Infrastruct Eng 2018;14(1):14–32. https://doi.org/10.1080/15732479.2017.1324883.
[23] Zhang Y, Tubaldi E, Macorini L, Izzuddin BA. Mesoscale partitioned modelling of masonry bridges allowing for arch-backfill interaction. Constr Build Mater 2018;173:820–42. https://doi.org/10.1016/j.conbuildmat.2018.03.272.
[24] Tubaldi E, Minga E, Macorini L, Izzuddin BA. Mesoscale analysis of multi-span masonry arch bridges. Eng Struct 2020;225:111137. https://doi.org/10.1016/j.engstruct.2020.111137.
[25] Stablon T, Sellier A, Domede N, Plu B, Dieleman L. A numerical tool for masonry arch bridges assessment. In: 9th World congress on railway research. 9; 2011 [Online]. Available, https://www.sparkrail.org/Lists/Records/DispForm.aspx?ID=3384.
[26] Silva R, Costa C, Arêde A. Nonlinear analysis of a multispan stone masonry bridge under railway traffic loading. In: Arêde A, Costa C, editors. Proceedings of ARCH 2019 9th international conference on arch bridges. Springer Nature Switzerland; 2020. p. 119–27. https://doi.org/10.1007/978-3-030-29227-0_8.
[27] Kerr T, O'Flaherty T. A numerical analysis of stone masonry arch bridges and structural backing. Civ Eng Res Irel 2020;(2) [Online]. Available, https://sword.cit.ie/ceri/2020/2/2.
[28] Minga E, Macorini L, Izzuddin BA. Enhanced mesoscale partitioned modelling of heterogeneous masonry structures. Int J Numer Methods Eng 2018;113(13):1950–71. https://doi.org/10.1002/nme.5728.
[29] Rouet F-H, et al. Scalability challenges of an industrial implicit finite element code. In: 2020 IEEE International parallel and distributed processing symposium (IPDPS); 2020. p. 505–14. https://doi.org/10.1109/IPDPS47924.2020.00059.
[30] Koric S, Gupta A. Sparse matrix factorization in the implicit finite element method on petascale architecture. Comput Methods Appl Mech Eng 2016;302:281–92. https://doi.org/10.1016/j.cma.2016.01.011.
[31] Franceschini A, Paludetto Magri VA, Mazzucco G, Spiezia N, Janna C. A robust adaptive algebraic multigrid linear solver for structural mechanics. Comput Methods Appl Mech Eng 2019;352:389–416. https://doi.org/10.1016/j.cma.2019.04.034.
[32] Adams M. Evaluation of three unstructured multigrid methods on 3D finite element problems in solid mechanics. Int J Numer Methods Eng 2002;55(5):519–34. https://doi.org/10.1002/nme.506.
[33] Jokhio GA, Izzuddin BA. A dual super-element domain decomposition approach for parallel nonlinear finite element analysis. Int J Comput Methods Eng Sci Mech 2015;16(3):188–212. https://doi.org/10.1080/15502287.2015.1043163.
[34] Macorini L, Izzuddin BA. Nonlinear analysis of masonry structures using mesoscale partitioned modelling. Adv Eng Softw 2013;60–61:58–69. https://doi.org/10.1016/j.advengsoft.2012.11.008.
[35] Tubaldi E, Macorini L, Izzuddin BA. Three-dimensional mesoscale modelling of multi-span masonry arch bridges subjected to scour. Eng Struct 2018;165:486–500. https://doi.org/10.1016/j.engstruct.2018.03.031.
[36] Izzuddin BA, Jokhio GA. Mixed-dimensional coupling for parallel partitioned nonlinear finite-element analysis. J Comput Civ Eng 2017;31(3):04016062. https://doi.org/10.1061/(ASCE)CP.1943-5487.0000633.
[37] Silva R, Costa C, Arêde A. Numerical methodologies for the analysis of stone arch bridges with damage under railway loading. Structures 2022;39:573–92. https://doi.org/10.1016/j.istruc.2022.03.063.